Published in final edited form as:
Cancer Res. 2008 March 1; 68(5): 1407–1416. doi:10.1158/0008-5472.CAN-07-2953.

T-cadherin Supports Angiogenesis and Adiponectin Association with the Vasculature in a Mouse Mammary Tumor Model

Lionel. W. Hebbard[1,+], **Michelle Garlatti**[1,+,#], **Lawrence J.T. Young**[2], **Robert D. Cardiff**[2], **Robert G. Oshima**[1], and **Barbara Ranscht**[1,*]

1 *Burnham Institute for Medical Research, 10901 North Torrey Pines Road, La Jolla, CA 92037, USA.*

2 *Center for Comparative Medicine and Pathology Department, University of California, Davis, Davis CA 95616, USA.*

Abstract

T-cadherin delineates endothelial, myoepithelial and ductal epithelial cells in the normal mouse mammary gland, and becomes progressively restricted to the vasculature during mammary tumorigenesis. To test the function of T-cadherin in breast cancer, we inactivated the T-cadherin gene in mice and evaluated tumor development and pathology after crossing the mutation into the MMTV-polyoma virus middle T (PyV-mT) transgenic model. We report that T-cadherin deficiency limits mammary tumor vascularization and reduces tumor growth. Tumor transplantation experiments confirm T-cadherin's stromal role in tumorigenesis. In comparison with wild type MMTV-PyV-mT controls, T-cadherin-deficient tumors are pathologically advanced and metastasize to the lungs. T-cadherin is a suggested binding partner for high molecular weight forms of the circulating fat-secreted hormone adiponectin. We discern adiponectin in association with the T-cadherin-positive vasculature in the normal and malignant mammary gland and report that this interaction is lost in the T-cadherin null condition. This work establishes a role for T-cadherin in promoting tumor angiogenesis and raises the possibility that vascular T-cadherin - adiponectin association may contribute to the molecular cross-talk between tumor cells and the stromal compartment in breast cancer.

Keywords

T-cadherin; vasculature; mammary tumor

Introduction

The adhesive function of the classical cadherin cell adhesion molecules is well known to play a major role in maintaining tissue integrity. Loss of cadherin expression or function is associated with a loss of cellular and spatial control that characterises neoplasia (1-5). T-cadherin shares the ectodomain structure with the classical cadherins and is anchored to the membrane via a glycosyl phosphatidyl inositol moiety (6,7). Like the classical transmembrane cadherins, T-cadherin is capable of conferring calcium-dependent homophilic cell adhesion (7). T-cadherin (also called H-cadherin or cadherin-13 in humans) is implicated in diverse types of human cancers where gene expression is silenced through methylation (8-12). Indeed, down-

*Corresponding Author Tel: 858−646−3122 (direct line), 858−646−3100 extn.3243 (Administrative Assistant) Fax: 858−646−3197 contact: E-mail: ranscht@burnham.org.
[+]equally contributing authors
[#]Dr. Garlatti's current address: INSERM U490, 45, Rue des Saints Pères, 75270 Paris Cedex 06, France.

regulation in human mammary neoplasia together with the observation that human breast cancer cells forced to over- express T-cadherin show reduced growth in culture have led to the suggestion T-cadherin may act as a tumor suppresser (13).

T-cadherin is expressed in diverse organs and cell types during development and in adulthood. Homophilic interactions are implicated in nervous system development and blood vessel growth. In the nervous system, T-cadherin's distribution and function correlate with events of decreased adhesion, such as axon branching, defasciculation and repulsion (14,15). Similarly, T-cadherin is suggested in regulating adhesiveness of vascular cells (16-18). We noted abundant vascular T-cadherin expression in mouse tumors, including transgenic epithelial mammary tumors expressing the Neu oncogene or both Neu and vascular endothelial growth factor (VEGF) (19,20). We thus hypothesized a possible role for T-cadherin in tumor angiogenesis. T-cadherin is a suggested binding partner for hexameric and high molecular weight (HMW) forms of the fat-secreted, circulating hormone adiponectin (21). Adiponectin is much discussed as a regulator of metabolic and vascular functions (22) although its mode of operation and functions at the cellular and molecular level remain incompletely understood.

The aim for this current study was to determine the role of T-cadherin in breast cancer. We generated a null allele of T-cadherin in mice and challenged the phenotype of homozygous mutants in the MMTVPyV-mT transgenic mammary cancer model. We report that loss of T-cadherin limits angiogenesis of mammary tumors resulting in slower tumor growth, increased hypoxia and pulmonary metastases. This phenotype correlates with the loss of adiponectin associated with the tumor vasculature and increased levels in the circulation. This work is the first to report a function for T-cadherin in promoting tumor angiogenesis *in vivo* and to suggest a link between T-cadherin and the association of adiponectin with blood vessels that may influence cross-talk between tumor cells and the stromal compartment.

Materials and Methods

Animal models and tissue preparation

All experiments were performed in accordance with Burnham Institute for Medical Research Animal Research Committee guidelines. The generation of the T-cadherin null mice and biochemical characterization will be described elsewhere. Wild-type MMTV-PyV-mT mice, originally generated by Dr. William Muller, McGill University, Montreal, were obtained in the C57Bl/6 background through Dr. Leslie Ellies, University of California San Diego. T-cadherin-deficient MMTV-PyV-mT mice were derived in two mating steps; i) heterozygous male MMTV-PyV-mT mice were crossed with T-cadherin$^{-/-}$ female mice; and ii) male MMTVPyV-mT T-cadherin$^{+/-}$ progeny was crossed with T-cadherin$^{+/+}$ and T-cadherin$^{-/-}$ females to yield female MMTV-PyV-mT T-cadherin$^{+/+}$ and PyV-mT T-cadherin$^{-/-}$ mice. Genotypes were determined by PCR. T-cadFO R 5 ’-CTCTGAACAGGTAGTCGATAGCGACAGAC-3 ’ a n d T-c a d R E V 5 ’-CGGAGACACTGCCTGTGTTCTCATTG-3’ amplified a 120 bp DNA fragment representing the wild type allele. In the same reaction, the T-cadFOR primer and the neomycin cassette primer 5’-GCATCGCCTTCTATCGCCTTCTG-3’ amplified the 350 bp mutant DNA fragment (Fig. 1). Tumor development was checked by palpitation three times a week from 60 days of life and measured with digital calipers. Tumor volume was calculated (length × width^2)/2 and appearance, survival and growth curves were derived in Prism® using Log-Rank test and Linear Regression analyzes. Wild type MMTV-PyV-mT$^{Y315/322F}$ tumors were transplanted in the number four mammary glands as previously described (29,42). The T-cadherin mutation was back-bred onto the FVB background for seven generations and 13 female mice of each genotype were used as hosts. Mice were sacrificed when T-cadherin$^{+/+}$ and T-cadherin$^{-/-}$ MMTV-PyV-mT tumors or the T-cadherin$^{+/+}$ recipients of MMTV-PyV-mT$^{Y315/322F}$ tumors reached the institutionally set limit, or the mice were moribund. Hypoxia

was induced as previously described (43). The animals were housed in the Institute's vivarium in compliance with the Animal Research Committee.

Histology, immunohistochemistry and image analysis

Mice were sacrificed by CO_2 inhalation before removing mammary fat pads or tumors. One half of the tissue was fixed in 4% paraformaldehyde in phosphate-buffered saline (PBS) overnight, dehydrated, and embedded in paraffin. Sections were cut at 10 μm and stained with hematoxylin and eosin. For pathological evaluation, 88 tumors from 28 mice (14 from each genotype) were examined by Dr. Cardiff. The other half was snap-frozen in liquid nitrogen and sectioned frozen at 10 μm for immunohistochemical analysis. Sections were collected on slides, fixed in ice-cold acetone for 10 minutes and air-dried. Unspecific binding sites were blocked with Tris-buffered saline with 0.05% Tween20 (TBST) buffer containing 10% FCS. The generation and specificity of T-cadherin antibodies (Garlatti and Ranscht, unpublished data) will be described elsewhere. Antibodies to CD31 (clone 390, PharMingen), SMA-Cy3 (Sigma, clone 1A4), E-cadherin (Zymed, clone ECCD-2), phospho-histone-H3 (Ser10, Upstate cell signalling solutions), Acrp30 (adiponectin, PA1−054, Affinity Bioreagents™) and ß-tubulin (clone E7, derived by Michael Klymkowsky, University of Colorado, Boulder, from the Developmental Studies Hybridoma Bank, Iowa) were purchased from the indicated commercial sources. Hypoxia analyzes were performed with a commercial kit, HypoxyProbe™ (Chemicon). Sections were incubated with primary antibodies in TBST overnight. For immunofluorescence, donkey anti-rabbit streptavidin-Alexa-488 conjugate (Molecular Probes) was used to detect T-cadherin and phospho-histone-H3 antibodies and anti-rat streptavidin-Alexa-594 conjugate (Molecular Probes) to detect CD31 and E-cadherin antibodies. Secondary antibodies were applied for 30 minutes. Apoptotic cells were identified with a commercial terminal deoxynucleotidyl-transferase-mediated nick-labelling immunofluorescence staining kit (ApopAlert™ DNA fragmentation assay kit, BD Biosciences). For BrdU incorporation, mice were injected 0.01 ml/g bromodeoxyuridine (Amersham, GE Healthcare) two hours prior to sacrifice. Frozen tissue sections were treated with 2M HCl, neutralized with 0.1M borate buffer pH 8.5, and processed for detection with a BrdU specific antibody (Clone BU1/75 (ICRI), Oxford Biotechnology). Sections were counterstained with DAPI (Molecular Probes) for ten minutes and mounted in Fluorescent Mounting Medium (DAKO). Staining signals were analyzed by confocal microscopy (MRC-1024 MP Biorad), or by capturing images of constant exposure with a Spot camera (Diagnostic Incorporated) on a Zeiss Axiovert 405M microscope for analyses in Photoshop®. For tumor statistics, four random images of solid tumor from two sections of the largest tumor from each mouse were analyzed. CD31 and HypoxyProbe™ staining was related to tumor area. Vessel branch points were identified in CD31 stained sections and related to tumor surface area. Apoptotic and phospho-histone H3 positive cells were related to the total number of DAPI stained nuclei using ImagePro® software. Statistical analyses were performed with Prism® software using the students t test on all data sets. Statistics are expressed as mean ± standard error of the mean.

Mammary gland whole mounts

Number 4 mammary glands were processed overnight in Carnoy's fixative and stained in Carmine for several hours*. After dehydration in xylene, glands were mounted with Permount (Fisher Scientific). Images were collected using a Olympus™ dissecting microscope and ductal branching and neoplastic area were analyzed using ImagePro® software.

*http://mammary.nih.gov/tools/histological/Histology/index.html#a1

Retinal Staining

Retinal neovascularization was induced by sequential exposure of P7 old mice to 75% oxygen followed by normoxic conditions (43). Eyes were removed from euthanized 17-day-old mice dissected, flat-mounted and permeabilized in PBS containing 10% fetal bovine serum and 0.1% Triton X-100 (PBSFT) overnight. Retinae were stained with FITC-labeled *Bandeiraea simplicifolia* lectin 1 isolectin B4 (VECTOR Laboratories) in PBSFT overnight, washed five times for one hour each and mounted in Moviol. Image analyses of retinal quadrants were performed with ImagePro® software from retinae of 6 mice for each genotype from two separate litters. Retinal glomeruli and vessel branch points were manually counted.

Immunoblotting

Tissues were lysed in RIPA buffer (50 mM Tris, pH 7.5, 150 mM NaCl, 1% NP40, 0.5% sodium deoxycholate, 0.1% SDS, 2mM sodium orthovanadate, 50 mM NaFl, 1mM sodium molybdate, 40 mM ß-glycero-phosphate, 1mM PMSF and 1/100 protease inhibitor cocktail, SIGMA, P8340), mechanically dissociated by sonication and centrifuged at 14,000 RPM for 10 min at 4°C. Thirty μg supernatant protein were loaded per lane and separated on SDS-PAGE gels under reducing conditions. T-cadherin, adiponectin and ß-tubulin were detected on blots with specific antibodies and the ECL Western Detection Kit (Amersham Biosciences). Adiponectin was analyzed under non-reducing conditions.

Results

T-cadherin delineates the vasculature in the mammary gland and mammary tumors

As we used the mammary gland as our experimental model, we first established the distribution of T-cadherin in wild-type mouse virgin breast tissue. Immunohistochemistry distinguished prominent T-cadherin expression on the apical surfaces of the polarized ductal mammary epithelium (Fig. 1A, a and e) and on CD31-positive endothelial cells (Fig. 1A, b and c). T-cadherin was also observed on the myoepithelium identified by smooth muscle actin (SMA) expression (Fig. 1A, f and g). The histological structure of the glands can be appreciated in Fig. 1A, d and h. Thus, T-cadherin delineates the myopepithelium, epithelium and endothelium of virgin mouse mammary glands.

Generation and overall phenotype of T-cadherin-deficient mice

To test the *in vivo* functions of T-cadherin, we generated mice deficient for T-cadherin gene expression. The generic targeting vector was created by insertion of the *neomycin* cassette into the Xho1-restriction site created within exon 5 of the T-cadherin gene by site-directed mutagenesis (Fig. 1B). Exon 5 encodes amino acids 161−210 within the T-cadherin extracellular domain 1. After homologous recombination in embryonic stem cells, germline chimeras were generated. Southern blotting (data not shown) and amplification of mutant DNA by the polymerase chain reaction (Fig. 1C) verified the homologous recombination event. The T-cadherin null mice were viable and fertile. Upon first inspection, their phenotype was indistinguishable from their wild type counterparts, including the lack of spontaneous tumor formation over a normal life span. Western blot analysis confirmed abundance of both the mature 100 kD T-cadherin protein and the 130 kD unprocessed precursor in the normal virgin mammary gland (Fig. 1D). To address if T-cadherin is required for normal mammary gland development, we examined the ductal patterning of virgin female T-cadherin$^{+/+}$ and T-cadherin$^{-/-}$ fat pads by carmine staining of whole-mounted glands. We observed no overt differences between genotypes in the degree of mammary ductal growth and branching (Supplemental Fig. 1). Moreover, sexually mature females deficient for T-cadherin produced and nourished multiple rounds of normal-sized litters (data not shown). Thus, mammary gland development and function appear to proceed normally in the absence of T-cadherin.

T-cadherin-deficiency restricts tumor growth in the MMTV-PyV-mT transgenic model

Since T-cadherin has been implicated in breast cancer in humans, we sought to establish a mouse model for examining the role of T-cadherin in mammary cancer. To accomplish that, we generated T-cadherin-deficient, tumor bearing mice by crossing the T-cadherin mutation into syngeneic C57Bl/6 transgenic mice expressing the polyoma virus middle T antigen from the mouse mammary tumor virus promoter (MMTV-PyV-mT) (23). The MMTV-PyV-mT mouse model is fast and reliable. Females form hyperplasias with hundred percent penetrance and display four identifiable mammary tumor stages classified as benign *in situ* proliferative lesions to invasive carcinomas with a high frequency of distant metastases (24,25). These stages mimic the expression of bio-markers characteristic of human mammary tumors with poor prognosis (26). We first examined the expression of T-cadherin during epithelial-mesenchymal transition in wild-type MMTV-PyV-mT tumors. At 85 days of life, T-cadherin was strongly expressed in the CD31-positive endothelium (data not shown) and in E-cadherin-labeled, polarized ductal epithelial cells and developing neoplasias (Fig. 2A, a-c). Contrastingly, developed cancers displayed decreased or no T-cadherin tumor cell-expression. In both early and advanced tumors, T-cadherin delineated the CD31-positive vasculature (Fig. 2A, e-g). Panels d and h of Fig. 2A depict the histological structure of the normal ductal, hyperplastic epithelium, and the appearance of advanced MMTV-PyV-mT tumors, respectively. Western blot analysis confirmed the significant reduction in T-cadherin levels in wild type MMTV-PyV-mT mammary tumors in relation to the normal wild type mammary gland (Fig.2B). No T-cadherin protein was produced in T-cadherin null mouse MMTV-PyV-mT tumors (Fig. 2B)

To test if the mutation affected overall tumor onset, growth and progression, we examined T-cadherin-deficient and wild type MMTV-PyV-mT transgenic mice for palpable tumors three times a week, starting at 60 days of age. Mammary tumors were detected in wild-type MMTV-PyV-mT mice with a median onset of 96.5 days. In the T-cadherin mutants, tumor growth was delayed by 10 days showing a median onset of 106.5 days ($P = 0.0268$; Fig. 3A). Monitoring the degree of neoplastic growth in both genotypes in whole mounts of number four fat pads at 85 days of life, i.e. before tumors were palpable in the wild-type condition (Fig. 3B, a and b), revealed a three-fold reduction of the area covered by neoplastic growth in the T-cadherin$^{-/-}$ MMTV-PyV-mT mice in comparison with the wild-type ($16.74 \pm 2.254\%$, for T-cadherin$^{+/+}$; $5.413 \pm 1.627\%$, for T-cadherin$^{-/-}$; $n = 9$ for both genotypes, $P = 0.0009$; Fig. 3B, c). T-cadherin-deficient MMTV-PyV-mT mice also survived their wild-type counterparts by an average of 18.5 days: The median survival time was 151 days for the wild-type and 169.5 days for the T-cadherin mutant mice ($P = 0.0008$; Fig. 3C). Consistently, the growth kinetics for the two largest tumors in each animal differed significantly between genotypes ($P < 0.0001$; Fig. 3D). These data establish that T-cadherin deficiency delays onset and restricts growth of mouse mammary tumors.

Limited vascularization in T-cadherin-deficient mammary tumors

To define the cellular events leading to restricted tumor growth in the T-cadherin-deficient mice, we examined mutant and wild type MMTV-PyV-mT tumors for differences in cell proliferation, blood vessel density, apoptotic rates, and hypoxia. First, since T-cadherin can affect cell cycle progression (27), we examined the proliferative potential of wild type and T-cadherin-deficient tumors. Bromodeoxyuridine incorporation (data not shown) and immunostaining for phosphorylated histone revealed no overt changes in the proliferative potential of tumor cells between genotypes (Fig. 4A, a-c). Second, as T-cadherin is prominent in the tumor vasculature (19,20), we investigated the vascular coverage of MMTV-PyV-mT tumors in both genotypes. CD31 immunostaining detected a 31% reduction in endothelial cell density in T-cadherin$^{-/-}$ MMTV-PyV-mT tumors as compared to the wild type (Fig. 4B, a-c; $5.816 \pm 0.4326\%$ for T-cadherin$^{+/+}$ versus $4.004 \pm 0.3110\%$ for T-cadherin$^{-/-}$, $P = 0.0022$). Vessel branching was reduced by 45% in the null condition (Fig. 4B, a, b and d; 77.57 ± 3.446

branch points for T-cadherin$^{+/+}$ and 42.28 ± 2.531 for T-cadherin$^{-/-}$; P < 0.0001). These results indicate a function for T-cadherin in tumor neovascularization. To obtain further evidence for the suggested pro-angiogenic role of T-cadherin, we assessed neovascularization in the retina after hypoxia (43). Flat-mounted retinae from wild type and T-cadherin null mice exposed to hypoxia were examined for vascular glomeruli, highly proliferative clusters of tortuous vessels produced in response to angiogenic stimuli, and vessel branching. Quantification of blood vessels labelled with endothelial cell-specific *Bandeiraea simplicifolia* lectin 1 isolectin B4 (BSL1-B4) revealed a 63% reduction of vascular glomeruli in T-cadherin$^{-/-}$ retinae as compared to the wild type (Supplemental Fig. 2A-C; T-cadherin$^{+/+}$ = 95.0 ± 7.0 and T-cadherin$^{-/-}$ = 35.5 ± 4.5 glomeruli; P<0.0001). Furthermore, we observed a 53% reduction of vascular branch points in the T-cadherin null condition (Supplemental Fig. 2D; T-cadherin$^{+/+}$ = 639.3 ± 29.07 and T-cadherin$^{-/-}$ = 299.3 ± 11.72 branch points, P<0.0001). These data further support a role for T-cadherin in promoting neovascularization *in vivo*. Lastly, since limited blood supply may starve MMTV-PyV-mT tumors, we examined apoptosis by staining for DNA strand breaks by terminal deoxynucleotidyl transferase Biotin-dUTP nick end labeling (TUNEL). Our analyses revealed a 6-fold increase in apoptotic nuclei in T-cadherin$^{-/-}$ MMTV-PyV-mT tumors (10.24 ± 3.105%) over the corresponding wild-type (1.588 ± 0.4696%, P = 0.0106; Fig. 4C, a-c). Consistent with the increase of apoptosis, staining with HypoxyProbe™indicated a three-fold significant increase in oxygen-deprived areas in T-cadherin$^{-/-}$ MMTV-PyV-mT tumors (7.002 ± 2.090%) versus wild-type (2.064 ± 0.7181%, Fig. 4D, a-c, P = 0.0401; panels d and e represent respective examples of the T-cadherin$^{+/+}$ and T-cadherin$^{-/-}$ MMTV-PyV-mT tumor pathology). These results, combined with the observation that T-cadherin-deficiency limits hypoxia-induced retinal angiogenesis, suggest that loss of T-cadherin limits tumor neovascularization and causes hypoxia that in turn restricts tumor cell survival.

Altered pathology and metastatic potential of T-cadherin-deficient MMTV-PyV-mT tumors

To characterize the effects of the T-cadherin mutation on mammary tumors, we compared the tumor pathology between genotypes. Histology of Hematoxilin & Eosin-stained sections revealed an unexpected and dramatic change in aggressiveness and metastatic rate of T-cadherin-deficient tumors. Wild-type MMTV-PyV-mT tumors showed the established range of polyoma middle T-induced mammary hyperplasias and tumor phenotypes in the C57Bl/6 background (28) with a predominance of adenocarcinomas (44/45 tumors) with a mixture of papillary and adenosquamous variants (Fig. 5A, a and c). One myoepithelioma was found. The MMTV-PyV-mT-induced tumors in the T-cadherin null condition differed from the wild-type cohort with the appearance of a unique poorly-differentiated tumor phenotype (Fig. 5A, b and d) in 8 of the 14 animals sampled, and in 13 of the 43 (30%) tumor samples (Supplemental Table 1). The poorly-differentiated tumors were composed of expansile nodular and solid cell masses with large pleomorphic hyperchromatic nuclei and scanty amphophilic cytoplasm. These cells did not form glands, papillae or squamous areas that are characteristic of the better-differentiated, wild-type MMTV-PyV-mT tumors. T-cadherin-deficient tumors often displayed juxtaposed regions of high mitotic rates and tumor necrosis, in-line with the documented increase in hypoxia and decrease in tumor vascularization.

All of the T-cadherin$^{-/-}$ MMTV-PyV-mT tumors developed pulmonary metastases in the C57Bl/6 background (Fig. 5A, e and f). In contrast, no metastatic growth was discernable in the wild type condition (Supplemental Table 2). The lung metastatic rate in the MMTV-PyV-mT mouse model is known to depend on the genetic background, and our observation that wild-type MMTV-PyV-mT tumors show few or no metastases in the C57Bl/6 strain is in agreement with previous reports (25, 28). T-cadherin null MMTVPyV-mT tumors acquired definitive metastatic properties as the perimeter of the pulmonary metastases was devoid of an endothelial border, and metastases were not lodged in the vasculature (Fig. 5A, g). In further

support of the altered tumor phenotype, the hematoxylin:eosin ratio in sections from T-cadherin$^{+/+}$ and T-cadherin$^{-/-}$ MMTV-PyV-mT tumors showed a significant shift in aggressive pathology (increase of eosin-stained areas) in the T-cadherin-deficient condition (Fig. 5A, h, 65.35 ± 2.435% for T-cadherin$^{+/+}$ and 35.96 ± 2.556 for T-cadherin$^{-/-}$; P<0.0001).

T-cadherin affects tumor growth as a stromal factor

With the reduction of pathological neovascularization in T-cadherin-deficient MMTV-PyV-mT tumors and the concomitant increase in tumor de-differentiation, we next distinguished if T-cadherin exerts cell autonomous and non-autonomous effects on tumor growth. To accomplish that, we transplanted wild type MMTV-PyV-mT tumors into mammary fat pads of FVB syngeneic wild-type and T-cadherin-deficient hosts. The switch of background was necessary as C57Bl/6 MMTV-PyV-mT tumors grow poorly after transplantation into syngenetic hosts. Moreover, wild-type MMTV-PyVmT tumors in the FVB background are more invasive than in the C57Bl/6 mouse strain. Thus, we used the non-metastatic variant MMTV-PyV-mT$^{Y315/322F}$ (29) for transplantation into mammary fat pads. Transplanted tumors were palpable in wild type hosts at 23 days, and with a one-week delay, at 30 days, in T-cadherin null recipients. Tumor growth kinetics was significantly reduced in the T-cadherin-deficient background (Fig. 5B; P = 0.000196 by linear regression analysis). Accordingly, the final MMTV-PyV-mT$^{Y315/322F}$ tumor weight in T-cadherin null mice was reduced by a factor of three in comparison to the wild-type (Fig. 5C; 956.5 ± 237.4 mg, n=22 for T-cadherin$^{+/+}$ and 345.3 ± 58.45 mg, n=20 for T-cadherin$^{-/-}$ hosts; p = 0.0215). Pathological analysis established that the donor papillary adenocarcinoma tumor pathology was preserved in hosts of both genotypes, albeit tumors remained small and often formed papillary cysts in the absence of T-cadherin (Fig. 5D, a and b; Supplemental Table 3). These data support a role of T-cadherin in the tumor microenvironment in line with the concept that T-cadherin regulates tumor vascularization.

T-cadherin ablation disrupts the association of adiponectin with the vasculature

With T-cadherin regulating neovascularization *in vivo*, the primary question arising from our studies is: How does T-cadherin regulate blood vessel growth? T-cadherin is a binding partner for the hexameric and HMW forms of adiponectin (21) and adiponectin is implicated in vascular functions (30,31). To gain initial insights into the possible cross-talk between these molecules *in vivo*, we examined the expression of adiponectin in wild type and T-cadherin-deficient mouse mammary tumors by immunohistochemistry. In wild type virgin mammary glands (data not shown) and MMTV-PyV-mT tumors, adiponectin was detected in association with the CD31-positive vasculature (Fig. 6A, a-c). In contrast, in T-cadherin null tumors, no specific signal was evident for adiponectin in any structure (Fig. 6A, e-g). Examination of the serum from mice of both genotypes revealed a dramatic upregulation of adiponectin levels in the T-cadherin null condition (Fig. 6B). Taken together these first *in vivo* observations link the expression of T-cadherin to a role in sequestering adiponectin to the vasculature where this interaction could contribute to regulating vascular functions.

Discussion

By generating and analyzing a T-cadherin-deficient mouse model of mammary cancer, we have revealed an unprecedented role for T-cadherin in tumor angiogenesis. T-cadherin is expressed on epithelial, myoepithelial and some endothelial cells in virgin mouse mammary tissue, and down-regulated from epithelial cells during development of luminal epithelial tumors. Thus, T-cadherin becomes progressively confined to the vasculature during tumorigenesis. The restricted vascular expression of T-cadherin in the MMTV-PyV-mT model replicates our observations in MMTV-Neu induced mouse tumors (19) and is similar to the situation in human cancers, including those of the breast (8-13). As T-cadherin expression is

progressively lost from epithelial cells during mammary tumorigenesis, the T-cadherin-deficient PyV-mT model can only assess a limited range of changes and leaves open the role of T-cadherin in the tumor cells. We report that genetic inactivation of T-cadherin does not accelerate tumorigenesis or result in formation of spontaneous tumors as might be expected if T-cadherin acted as a bona fide tumor suppressor. Rather, the loss of T-cadherin delays MMTV-PyV-mT tumor formation, retards growth and increases metastases. We attribute this phenotype to a major function of T-cadherin in tumor angiogenesis. The T-cadherin$^{-/-}$ MMTVPyV-mT tumors are significantly less vascularized than those from corresponding wild type mice. The null mice develop no life-threatening vascular defects during embryogenesis, but show specific impairments in pathological neovascularization of mammary tumors and hypoxia-induced blood vessel remodeling of the retina. Reduced endothelial cell density and increased hypoxia in T-cadherin-deficient MMTV-PyV-mT tumors together with the observation that T-cadherin in the host microenvironment is needed for supporting growth of MMTV-PyV-mT tumors after transplantation, suggest an important role for T-cadherin in pathological neovascularization. We correlate the association of adiponectin with the tumor vasculature with T-cadherin's pro-angiogenic role and suggest a link between T-cadherin's vascular expression, adiponectin binding capability and tumor neovascularization.

An unexpected outcome of the current study was that T-cadherin$^{-/-}$ MMTV-PyV-mT tumors attain a more malignant pathology and metastatic potential even though overall tumor growth is limited. The metastatic rate of MMTV-PyV-mT mouse tumors is known to be influenced by the genetic background (25), and is low in the C57Bl/6 strain used for the current study (See Supplemental Table 2). As T-cadherin is progressively lost from the ductal epithelium during normal tumorigenesis, how can the ablation of T-cadherin affect tumor cell invasion and metastasis? Two explanations are possible. First, the increased metastatic potential results from the disruption of T-cadherin-mediated adhesive interactions that prevents straying of neoplastic epithelial cells. This model assumes that low T-cadherin levels normally present on PyV-mT tumor cells are sufficient to restrain cells to the primary tumor mass and inhibit metastatic spreading. This suggestion would need to be tested in a gain-of-function genetic model. Alternatively, the limited blood supply of T-cadherin-deficient tumors increases hypoxia and changes in the tumor pathology (32,33). Hypoxia is well known to be associated with a poor clinical outcome of invasive human breast carcinoma (34), and T-cadherin-deficient tumors present with reduced blood vessel density, enhanced apoptosis, and enlarged hypoxic and necrotic regions. The metastases in T-cadherin$^{-/-}$ MMTV-PyV-mT mice are not associated with endothelial cells and thus may represent section for an epithelial-meschenymal type transition.

T-cadherin has at least two activities that may influence angiogenesis. First, T-cadherin confers homophilic binding between cells (7), and this engagement is reported to decrease adhesion, enhance migration and induce proliferation of endothelial cells (16,17). Moreover, ectopic T-cadherin expression in the capillary microenvironment *in vivo* repulses blood vessels and stops their growth (35). Thus, inactivation of T-cadherin *in vivo* might be expected to increase vascularization. However, the data presented here from the mouse null model do not support a restrictive role for T-cadherin in blood vessel growth *in vivo*. Rather, the T-cadherin null mice show limited angiogenic responses suggesting a function for T-cadherin in supporting angiogenesis. Our work thus leaves open if the repulsive, homophilic binding function of T-cadherin plays into the complex interactions during angiogenesis *in vivo*. Secondly, T-cadherin is a binding protein for the hexameric and HMW forms of adiponectin (21), the predominant active forms in serum (36). We find that adiponectin is sequestered to the vasculature in a T-cadherin-dependent manner and levels are dramatically increased in serum. Thus, T-cadherin may serve as a major adiponectin repository. The functions of adiponectin in the vasculature remain controversial, both positive and negative actions on blood vessel growth are reported (30,31). Linking T-cadherin and adioponectin functions at a mechanistic level is thus a primary

research task. Because of its membrane attachment through a glycosylphosphatidyl inositol moiety, T-cadherin alone is insufficient to act as a receptor transducing signals elicited by adiponectin binding. Thus, we favour a model in which T-cadherin signals through associated molecules that perhaps provide a link with adiponectin- or other vascular receptors. One conceivable role for T-cadherin as an adiponectin binding protein includes sequestering adiponectin-associated growth factors, such as PDGF-BB, bFGF, HB-EGF and Trombospondin-1 (37,38). These factors exert important roles in establishing functional and stable vascular networks (39-41), and the T-cadherin-dependent accumulation of adiponectin may regulate their availability upon signals eliciting vascular responses. Irrespective of the mechanism, the work reported here establishes that T-cadherin regulates retinal and tumor angiogenesis and is responsible for sequestering adiponectin to the vasculature. These studies thus open new avenues for unravelling the molecular complexity of the vascular response under challenging physiological conditions.

Supplementary Material

Refer to Web version on PubMed Central for supplementary material.

Acknowledgements

We thank Dr. William Muller (McGill University, Montreal, Canada), and Dr. Erkki Ruoslahti (Burnham Institute for Medical Research Santa Barbara, CA) for insightful comments and encouragement throughout this work. Dr. Muller also provided the MMTV-PyV-MT and MMTV-PyV-mT$^{Y315/322F}$ transgenic mice, and Drs. Christopher Hug and Harvey Lodish (Whitehead Institute, Cambridge, MA) inspired the investigation of adiponectin levels in serum. We gratefully acknowledge Ms. Xuandao Duong-Polk for mouse breeding and genotyping, Dr. Edward Monosov and Ms. Jennifer Meerloo for assistance with image analysis, Ms. Robbin Newlin for the preparation of hematoxylin and eosin stained sections, and Mr. Robert Munn for the pathology images. The research in this publication was supported by NIH grant HD25938 and DOD grant W81-XWH-04-1-0574 for BR, NCI grant CA 098778 for RGO and RDC, and NCI grants CA089140 and U01 CA105490-01, DOD DAMD17-02-1-0694 for RDC. LWH is a recipient of a 2005 Fishman Award.

References

1. Christofori G, Semb H. The role of the cell-adhesion molecule E-cadherin as a tumor- suppressor gene. Trends Biochem Sci 1999;24:73–6. [PubMed: 10098402]
2. Hermiston ML, Gordon JI. Inflammatory bowel disease and adenomas in mice expressing a dominant negative N-cadherin. Science 1995;270:1203–7. [PubMed: 7502046]
3. Vleminckx KL, Deman JJ, Bruyneel EA, et al. Enlarged cell-associated proteoglycans abolish E-cadherin functionality in invasive tumor cells. Cancer Res 1994;54:873–7. [PubMed: 8313373]
4. Watabe M, Nagafuchi A, Tsukita S, Takeichi M. Induction of polarized cell-cell association and retardation of growth by activation of the E-cadherin-catenin adhesion system in a dispersed carcinoma line. J Cell Biol 1994;127:247–56. [PubMed: 7929567]
5. Radice GL, Ferreira-Cornwell MC, Robinson SD, et al. Precocious mammary gland development in P-cadherin-deficient mice. J Cell Biol 1997;139:1025–32. [PubMed: 9362520]
6. Ranscht B, Dours-Zimmermann MT. T-cadherin, a novel cadherin cell adhesion molecule in the nervous system lacks the conserved cytoplasmic region. Neuron 1991;7:391–402. [PubMed: 1654948]
7. Vestal DJ, Ranscht B. Glycosyl phosphatidylinositol--anchored T-cadherin mediates calcium-dependent, homophilic cell adhesion. J Cell Biol 1992;119:451–61. [PubMed: 1400585]
8. Fiegl H, Millinger S, Goebel G, et al. Breast cancer DNA methylation profiles in cancer cells and tumor stroma: association with HER-2/neu status in primary breast cancer. Cancer Res 2006;66:29–33. [PubMed: 16397211]
9. Kim JS, Han J, Shim YM, Park J, Kim DH. Aberrant methylation of H-cadherin (CDH13) promoter is associated with tumor progression in primary nonsmall cell lung carcinoma. Cancer 2005;104:1825–33. [PubMed: 16177988]

10. Lewis CM, Cler LR, Bu DW, et al. Promoter hypermethylation in benign breast epithelium in relation to predicted breast cancer risk. Clin Cancer Res 2005;11:166–72. [PubMed: 15671542]

11. Hibi K, Kodera Y, Ito K, Akiyama S, Nakao A. Methylation pattern of CDH13 gene in digestive tract cancers. Br J Cancer 2004;91:1139–42. [PubMed: 15292927]

12. Toyooka KO, Toyooka S, Virmani AK, et al. Loss of expression and aberrant methylation of the CDH13 (H-cadherin) gene in breast and lung carcinomas. Cancer Res 2001;61:4556–60. [PubMed: 11389090]

13. Lee SW. H-cadherin, a novel cadherin with growth inhibitory functions and diminished expression in human breast cancer. Nat Med 1996;2:776–82. [PubMed: 8673923]

14. Fredette BJ, Miller J, Ranscht B. Inhibition of motor axon growth by T-cadherin substrata. Development 1996;122:3163–71. [PubMed: 8898229]

15. Fredette BJ, Ranscht B. T-cadherin expression delineates specific regions of the developing motor axon-hindlimb projection pathway. J Neurosci 1994;14:7331–46. [PubMed: 7996179]

16. Ivanov D, Philippova M, Allenspach R, Erne P, Resink T. T-cadherin upregulation correlates with cell-cycle progression and promotes proliferation of vascular cells. Cardiovasc Res 2004;64:132–43. [PubMed: 15364621]

17. Ivanov D, Philippova M, Tkachuk V, Erne P, Resink T. Cell adhesion molecule T-cadherin regulates vascular cell adhesion, phenotype and motility. Exp Cell Res 2004;293:207–18. [PubMed: 14729458]

18. Philippova M, Ivanov D, Allenspach R, Takuwa Y, Erne P, Resink T. RhoA and Rac mediate endothelial cell polarization and detachment induced by T-cadherin. Faseb J 2005;19:588–90. [PubMed: 15703273]

19. Oshima RG, Lesperance J, Munoz V, et al. Angiogenic acceleration of Neu induced mammary tumor progression and metastasis. Cancer Res 2004;64:169–79. [PubMed: 14729621]

20. Wyder L, Vitaliti A, Schneider H, et al. Increased expression of H/T-cadherin in tumor-penetrating blood vessels. Cancer Res 2000;60:4682–8. [PubMed: 10987267]

21. Hug C, Wang J, Ahmad NS, Bogan JS, Tsao TS, Lodish HF. T-cadherin is a receptor for hexameric and high-molecular-weight forms of Acrp30/adiponectin. Proc Natl Acad Sci U S A Jun 21;2004 101:10308–13. [PubMed: 15210937]Epub 2004

22. Kadowaki T, Yamauchi T, Kubota N, Hara K, Ueki K, Tobe K. Adiponectin and adiponectin receptors in insulin resistance, diabetes, and the metabolic syndrome. J Clin Invest 2006;116:1784–92. [PubMed: 16823476]

23. Guy CT, Cardiff RD, Muller WJ. Induction of mammary tumors by expression of polyomavirus middle T oncogene: a transgenic mouse model for metastatic disease. Mol Cell Biol 1992;12:954–61. [PubMed: 1312220]

24. Lin EY, Jones JG, Li P, et al. Progression to malignancy in the polyoma middle T oncoprotein mouse breast cancer model provides a reliable model for human diseases. Am J Pathol 2003;163:2113–26. [PubMed: 14578209]

25. Lifsted T, Le Voyer T, Williams M, et al. Identification of inbred mouse strains harboring genetic modifiers of mammary tumor age of onset and metastatic progression. Int J Cancer 1998;77:640–4. [PubMed: 9679770]

26. Maglione JE, Moghanaki D, Young LJ, et al. Transgenic Polyoma middle-T mice model premalignant mammary disease. Cancer Res 2001;61:8298–305. [PubMed: 11719463]

27. Huang ZY, Wu Y, Hedrick N, Gutmann DH. T-cadherin-mediated cell growth regulation involves G2 phase arrest and requires p21(CIP1/WAF1) expression. Mol Cell Biol 2003;23:566–78. [PubMed: 12509455]

28. Ellies LG, Fishman M, Hardison J, et al. Mammary tumor latency is increased in mice lacking the inducible nitric oxide synthase. Int J Cancer 2003;106:1–7. [PubMed: 12794750]

29. Webster MA, Hutchinson JN, Rauh MJ, et al. Requirement for both Shc and phosphatidylinositol 3' kinase signaling pathways in polyomavirus middle T-mediated mammary tumorigenesis. Mol Cell Biol 1998;18:2344–59. [PubMed: 9528804]

30. Ouchi N, Kobayashi H, Kihara S, et al. Adiponectin stimulates angiogenesis by promoting cross-talk between AMP-activated protein kinase and Akt signaling in endothelial cells. J Biol Chem Oct 13;2004 279:1304–9. [PubMed: 14557259]Epub 2003

31. Brakenhielm E, Veitonmaki N, Cao R, et al. Adiponectin-induced antiangiogenesis and antitumor activity involve caspase-mediated endothelial cell apoptosis. Proceedings of the National Academy of Sciences of the United States of America 2004;101:2476–81. [PubMed: 14983034]
32. Yoon SO, Shin S, Mercurio AM. Hypoxia stimulates carcinoma invasion by stabilizing microtubules and promoting the Rab11 trafficking of the alpha6beta4 integrin. Cancer Res 2005;65:2761–9. [PubMed: 15805276]
33. Zhang L, Hill RP. Hypoxia enhances metastatic efficiency by up-regulating Mdm2 in KHT cells and increasing resistance to apoptosis. Cancer Res 2004;64:4180–9. [PubMed: 15205329]
34. Dales JP, Garcia S, Meunier-Carpentier S, et al. Overexpression of hypoxia-inducible factor HIF-1alpha predicts early relapse in breast cancer: Retrospective study in a series of 745 patients. Int J Cancer 2005;22:22.
35. Rubina K, Kalinina N, Potekhina A, et al. T-cadherin suppresses angiogenesis in vivo by inhibiting migration of endothelial cells. Angiogenesis 2007;10:183–95. [PubMed: 17486418]
36. Pajvani UB, Hawkins M, Combs TP, et al. Complex distribution, not absolute amount of adiponectin, correlates with thiazolidinedione-mediated improvement in insulin sensitivity. J Biol Chem 2004;279:12152–62. [PubMed: 14699128]
37. Wang Y, Xu LY, Lam KS, Lu G, Cooper GJ, Xu A. Proteomic characterization of human serum proteins associated with the fat-derived hormone adiponectin. Proteomics 2006;6:3862–70. [PubMed: 16767790]
38. Wang Y, Lam KS, Xu JY, et al. Adiponectin inhibits cell proliferation by interacting with several growth factors in an oligomerization-dependent manner. J Biol Chem Feb 25;2005 280:18341–7. [PubMed: 15734737]Epub 2005
39. Cao R, Brakenhielm E, Pawliuk R, et al. Angiogenic synergism, vascular stability and improvement of hind-limb ischemia by a combination of PDGF-BB and FGF-2. Nat Med Mar 31;2003 9:604–13. [PubMed: 12669032]Epub 2003
40. Pepper MS, Ferrara N, Orci L, Montesano R. Potent synergism between vascular endothelial growth factor and basic fibroblast growth factor in the induction of angiogenesis in vitro. Biochem Biophys Res Commun 1992;189:824–31. [PubMed: 1281999]
41. Ongusaha PP, Kwak JC, Zwible AJ, et al. HB-EGF is a potent inducer of tumor growth and angiogenesis. Cancer Res 2004;64:5283–90. [PubMed: 15289334]
42. Young, LJT. The cleared mammary fat pad and the transplantation of mammary gland morphological structures and cells.. In: I a A K A P Publishers. , editor. Methods in Mammary Gland Biology and Breast Cancer Research. Plenum Publishers; New York: 2000. p. 67-74.2000
43. Smith LE, Wesolowski E, McLellan A, et al. Oxygen-induced retinopathy in the mouse. Invest Ophthalmol Vis Sci 1994;35:101–11. [PubMed: 7507904]

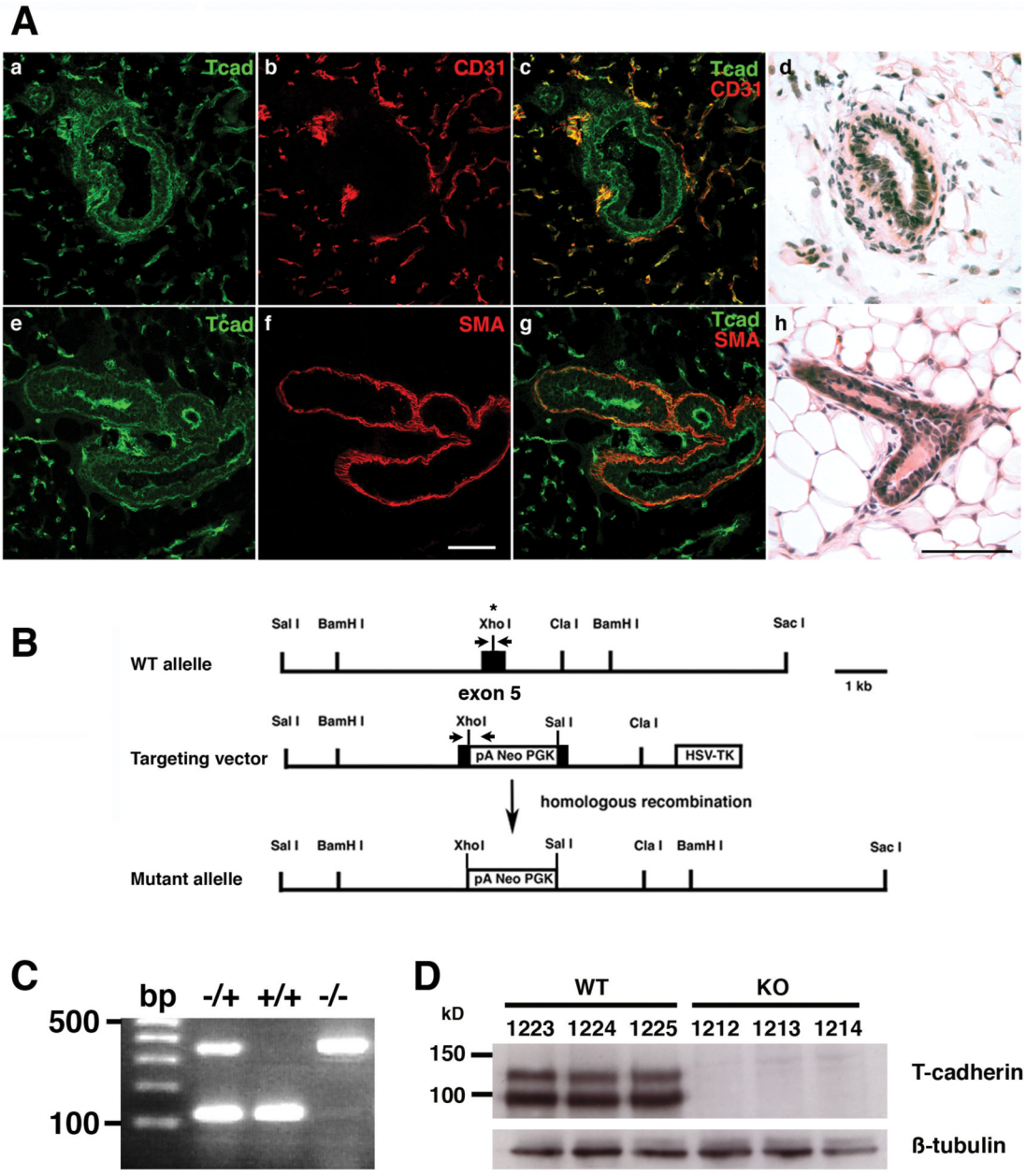

Figure 1. T-cadherin expression in the mouse mammary gland

A, in 7-week old virgin mouse mammary glands, T-cadherin (*a* and *e*) colocalizes with CD31 on endothelial cells (*b* and *c*) and with smooth muscle actin (SMA) on the myoepithelium (*f* and *g*). T-cadherin also delineates the mammary ductal epithelium where it is primarily localized apically. Representative cross-sections of ductal-epithelium are shown in panels (*d)* and (*h)*. Scale bars 50 μm. *B*, shows the gene targeting vector for generic ablation of T-cadherin in mice. The neomycin cassette was inserted into the Xho1 site (asterisk) introduced into exon 5 by point mutation. *C*, Genotypes were distinguished by PCR using forward and reverse primers indicated in Figure 1B to amplify the wild type 120 bp and the mutant 350 bp DNA fragments, respectively. D, Western blot analysis of three wild type mammary fat pads identifies a doublet representing the mature 100 kD T-cadherin protein and the 130 kD

precursor containing the proprotein region. No protein is detected in T-cadherin null mice. Equal loading is confirmed with anti-ß-tubulin antibodies.

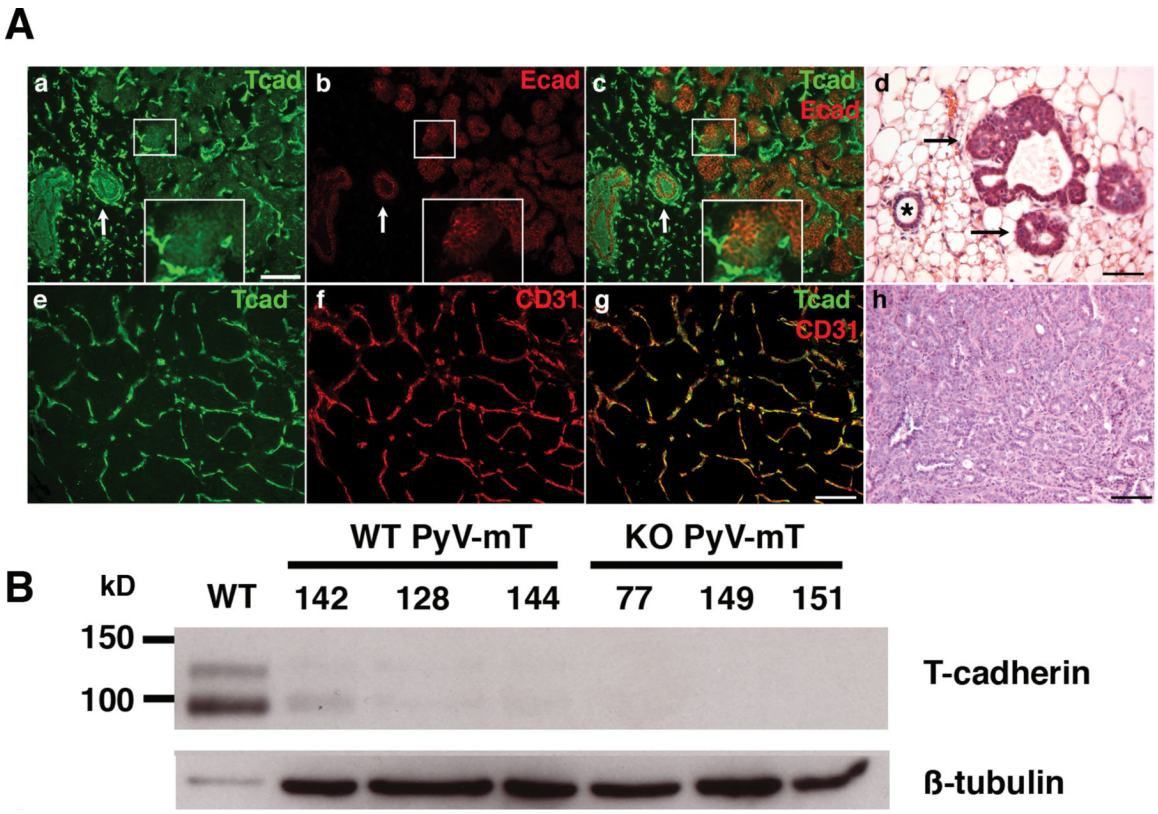

Figure 2. Expression of T-cadherin in the neoplastic mammary gland

A, in wild type MMTV-PyV-mT mammary fat pads at P85, T-cadherin *(a)* and E-cadherin (*b* and *c*), white arrows) delineate the normal ductal epithelium. Reduced levels of T-cadherin are detected on developing neoplasias (central white box and magnified image box, *(a)-(c)*). For comparison the pathology of a normal duct (asterisk) and developing neoplasias (black arrows) are illustrated in (d). Scale bars 50 μm. In developed wild-type MMTV-PyV-mT tumors, T-cadherin (*e*) is detected only on the CD31-positive vasculature (*f* and *g*). (*h*), represents the pathology of a T-cadherin$^{+/+}$ MMTV-PyV-mT tumor. Scale bars A-C 100 μm. *B*, Western blotting shows T-cadherin in the fat pads of T-cadherin$^{+/+}$ female mice, and its down-regulation in the MMTV-PyV-mT transgenic mammary gland. No T-cadherin protein is detected in breast tissue from T-cadherin null mice. Equal loading is confirmed with anti ß-tubulin antibodies.

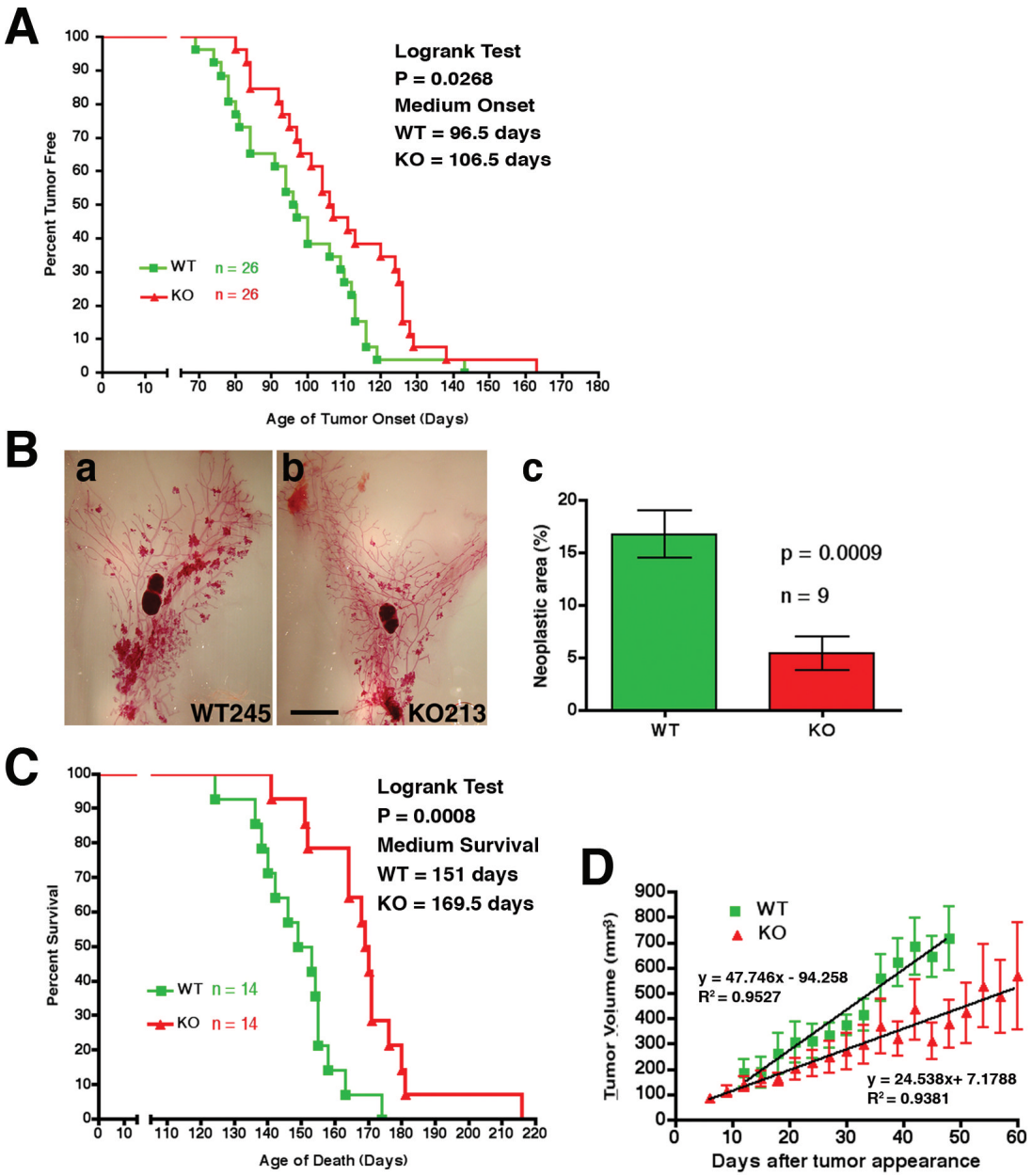

Figure 3. T-cadherin-deficient MMTV-PyV-mT tumors show restricted growth

A, time of initial tumor detection in T-cadherin$^{+/+}$ (ν) and T-cadherin$^{-/-}$ MMTV-PyV-mT (σ) transgenic mice is shown as a function of age. The median time of tumor detection is 96.5 days for the wild type and 106.5 days for the mutants (statistically significant by Logrank test; P = 0.0268). *B*, examples of whole mount number 4 mammary fat pads exhibiting MMTV-PyV-mT neoplastic growth at P85 in (*a*) T-cadherin$^{+/+}$ (245) and (*b*) T-cadherin$^{-/-}$ mice (213). Scale bar, 1 mm. Quantification of neoplastic area (*c*), revealed a nearly 3-fold reduction in the null mice (n = 9; P = 0.0009). *C*, T-cadherin$^{-/-}$ MMTV-PyV-mT mice extend their life span by 18.5 days as compared to their T-cadherin$^{+/+}$ counterparts. Median survival rates are indicated, and logrank tests indicate a statistically significant difference between genotypes (P = 0.0008). *D*, the mean tumor volume and standard error of the mean is shown as a function of elapsed time after first detection for the largest two tumors of 14 mice from each genotype. Trend lines were determined by linear regression analysis of the means in the Prism® statistical

program and established differences in the growth kinetics between T-cadherin$^{+/+}$ and T-cadherin$^{-/-}$ MMTV-PyV-mT mammary tumors; $P < 0.0001$.

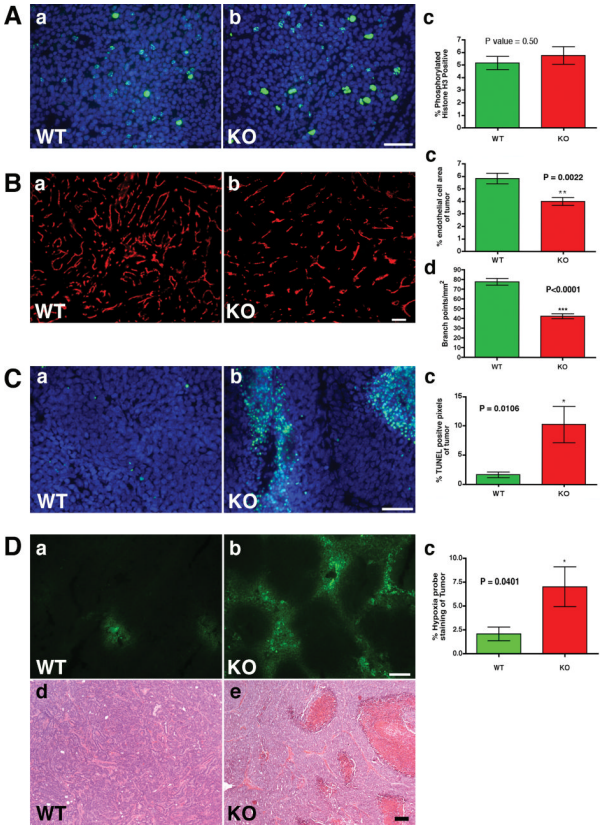

Figure 4. T-cadherin$^{-/-}$ MMTV-PyV-mT tumors show unchanged proliferation, reduced endothelial density, increased tumor cell apoptosis and enhanced hypoxia

A, phospho-Histone H3 labeling revealed no statistical differences in cell proliferation between T-cadherin$^{+/+}$ (*a*) and T-cadherin$^{-/-}$ (*b*) tumors. (*c*; P = 0.50). *B*, analysis of CD31 staining from T-cadherin$^{-/-}$ (*a*) and T-cadherin$^{+/+}$ (*b*) tumors staining shows a 31% reduction of endothelial cell coverage (*c*; P = 0.0022) and a 45% reduction of vessel branching (*d*; P<0.0001). *C*, TUNEL staining reveals a 6-fold increase in apoptotic tumor nuclei in T-cadherin$^{-/-}$ (*a*) over T-cadherin$^{+/+}$ (*b*) tumors. (*c*; P = 0.0106). *D*, immunofluorescence with a FITC-labeled Hypoxyprobe^{TM}-1 antibody showed a significant three-fold increase in hypoxic area from T-cadherin$^{-/-}$ (*a*) to T-cadherin$^{+/+}$ (*b*) tumors. (*c*; P = 0.0401). Representative images of T-cadherin$^{-/-}$ (*d*) to T-cadherin$^{+/+}$ (*e*) tumors are shown. Scale bars 50 μm.

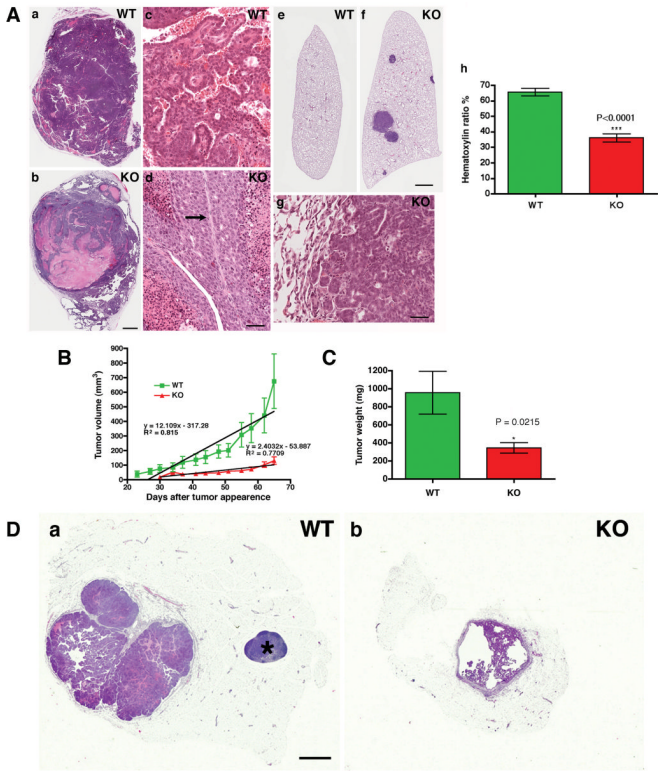

Figure 5. Poor differentiation and high metastatic potential of transgenic T-cadherin$^{-/-}$ MMTV-PyV-mT tumors, and limited MMTV-PyV-mT$^{Y315/322F}$ tumor growth after transplantation into T-cadherin-deficient hosts

A, examples of gross tumor pathology are shown: (*a*), T-cadherin$^{+/+}$ MMTV-PyV-mT tumor with complex solid and papillary carcinomas with prominent vessels; (*b*), three poorly differentiated, partially necrotic T-cadherin$^{-/-}$ MMTV-PyV-mT carcinomas and papillary tumors. Scale bar 1 mm. Magnified images of these tumors display glandular forms in differentiated (*c*) T-cadherin$^{+/+}$ tumors, and the poorly-differentiated pathology of necrotic (*d*) T-cadherin$^{-/-}$ tumors. Note the apoptosed cells on either side of the central blood vessel (arrow) in **(*d*)**. Scale bar 50 μm. Supplemental Table 1, presents the summary of tumor pathologies. Evaluation of the metastatic potential revealed that T-cadherin$^{+/+}$ MMTV-PyV-mT tumors metastasize poorly to the lungs (*e*; 14 mice), whereas all T-cadherin$^{-/-}$ tumor-bearing animals (*f*; 14 mice) show lung metastases. Magnified images of the lungs illustrate the invasive phenotype of T-cadherin$^{-/-}$ MMTV-PyV-mT tumor metastasis (*g*). Statistics in Supplemental Table 2, shows 6.1 ± 4.2 metastases per T-cadherin$^{-/-}$ MMTV-PyV-mT mouse and none in the wild-type. Quantitative evaluation of the hematoxylin/eosin ratio from mammary tumors shows that T-cadherin$^{-/-}$ MMTV-PyV-mT tumors exhibit poorly-differentiated pathology as compared to the T-cadherin$^{+/+}$ MMTV-PyV-mT condition (*h*; 65.35 ± 2.435% for wild-type and 35.96 ± 2.556% for mutant tumors; $P < 0.0001$). *B*, MMTV-PyV-mT$^{Y315/322F}$ tumors show delayed appearance and retarded growth after transplantation into T-cadherin$^{-/-}$ hosts (WT, n = 22 and KO, n = 20). Linear regression analysis shows significant differences in MMTV-PyV-mT$^{Y315/322F}$ tumor growth kinetics between T-cadherin$^{+/+}$ and T-cadherin$^{-/-}$ host environment ($P = 0.000196$). *C*, comparison of final tumor weights confirms a significant difference between genotypes ($P = 0.0215$). Supplemental Table 3, summarizes the pathology of T-cadherin$^{+/+}$ MMTV-PyV-mT$^{Y315/322F}$ tumors after transplantation into T-cadherin$^{+/+}$ and T-cadherin$^{-/-}$ mice. Donor pathology was maintained in both genotypes. *D*, examples of gross tumor pathology in T-cadherin$^{+/+}$ (*a*) and T-cadherin$^{-/-}$ (*b*) hosts are shown (scale bar 1 mm). The asterisk marks the lymphnode in (*a*)**.**

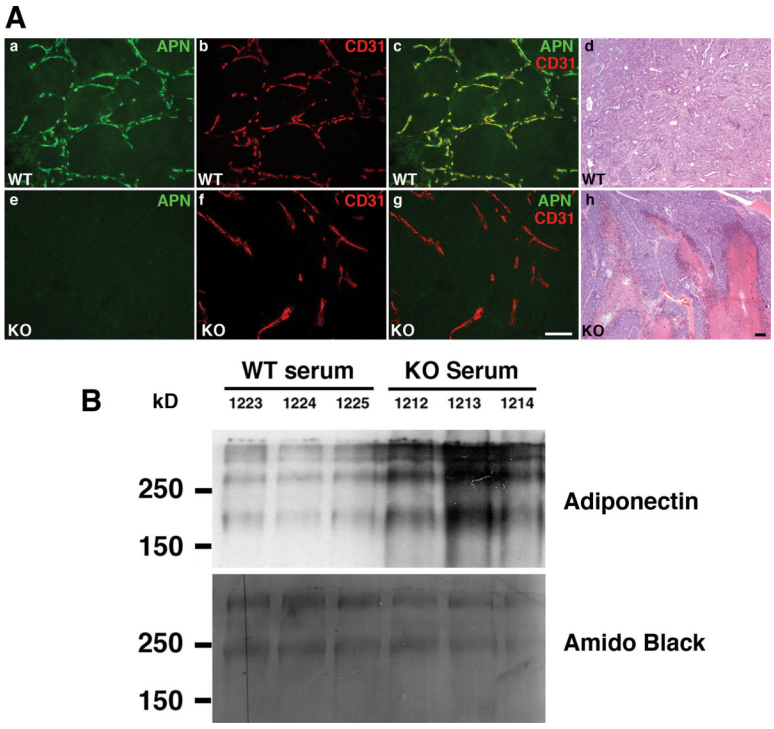

Figure 6. Adiponectin is displaced from the T-cadherin$^{-/-}$ MMTV-PyV-mT tumor vasculature and is upregulated in the serum

A, confocal analysis of T-cadherin$^{+/+}$ MMTV-PyV-mT tumors after staining for Adiponectin (APN) (*a*), and CD31 (*b)* shows colocalization to the vasculature (*c*). In T-cadherin$^{-/-}$ MMTV-PyV-mT tumors, adiponectin is not associated with the vasculature (*e-g*). Identical exposure times were used. Representative images of T-cadherin$^{+/+}$ and (*d*) T-cadherin$^{-/-}$ MMTV-PyV-mT (h) tumors are shown. Scale bars 50 μm. *B*, Western blot analysis for adiponectin. High molecular weight adiponectin is detected in one microliter serum from each of three T-cadherin$^{+/+}$ and three T-cadherin$^{-/-}$ mice. Levels are dramatically elevated in T-cadherin null mice. Staining for Amido Black is used as a loading control.